Supplemental Materials

Molecular Biology of the Cell

Fox et al.

SUPPLEMENTAL MATERIAL

SUPPLEMENTAL FIGURE LEGENDS

FIGURE S1: TOG domains show positional conservation in the array. (A-E) Identity matrices, comparing TOG domains within a protein (A, ch-TOG; B, Msps; C, Stu2) or across species (D, ch-TOG vs. Stu2; E, Msps vs. Stu2). Percent identity, based on the alignment presented in Figure 1C, is indicated in each cell with the corresponding number of aligned residues listed below. Percent identity is contoured from 0% (white) to 60% (red). 100% identity is shown in gray.

FIGURE S2: Individual Msps TOG domains are α-helical and have varying thermo-stability. (A) Above: domain architecture of *Drosophila* Msps; below: CD spectra of Msps TOG1 (blue), TOG2 (cyan), TOG3 (green), TOG4 (light green), and TOG5 (purple) at 23°C, pH 7.5 (3.7 μM). Spectra show minima at 208 and 222 nm, indicative of α-helical structure in each of the TOG domains. (B-F) CD melts of Msps TOG1 (B), TOG2 (C), TOG3 (D), TOG4 (E), and TOG5 (F). CD signal was monitored at 208 nm (dashed trace) and 222 nm (solid trace) in 1°C steps from 20°C to 94°C. The inflection points were 46.5°C, 64.5°C, 50.5°C, and 46.5°C for TOG1, TOG2, TOG3, and TOG4, respectively. TOG5 had no inflection point suggesting that the domain, as defined by the region exclusively spanning its six predicted HEAT repeats, is not stable. Experiments were performed in duplicate with data from single, representative experiments shown.

FIGURE S3: TOG4 protomer structures are similar within and across space groups. Pairwise structural alignment of human ch-TOG TOG4 determined in two different crystal forms (ch-TOG TOG4 SeMet, $P4_32_12$ (blue); ch-TOG TOG4 native, $P2_12_12_1$ protomer A (red), ch-TOG TOG4 native, $P2_12_12_1$ protomer B (green). Cα rmsd values are indicated below each alignment with the corresponding number of Cα atoms aligned.

FIGURE S4: The TOG4 structure is architecturally distinct from other XMAP215 TOG structures. Pairwise structural alignment matrix of XMAP215 family TOG domains: Stu2 TOG1 (dark blue), Stu2 TOG2 (cyan), Msps TOG2 (purple), Zyg-9 TOG3 (green), and Msps TOG4 (pink). Domains are shown in cartoon representation. Matrices in the lower right indicate the rmsd values (top) for the number of Cα atoms aligned (center), and the percent identity across the aligned region (bottom). (A) Pairwise structural alignment performed across HR A-F. (B) Pairwise structural alignment performed across HR A-C.

Figure S5: Msps TOG1-2 and TOG3-4 do not co-sediment with taxol-stabilized MTs. (A) MTs were pelleted at 100,000xg. 100% of the load (left panel) was observed in the pellet (right panel, right lane). A Msps TOG1-2 construct (residues 1-516) (B) and a TOG3-4-GFP construct (residues 582-1080, upper band; lower band is a TOG3-4-GFP degradation product) (C) were centrifuged in the presence and absence of taxol-stabilized MTs (left panels, load; right panel supernatant and pellets). Both constructs were observed in the supernatant alone indicating that the constructs, at the concentrations used, do not robustly bind and co-sediment with taxol-stabilized MTs. L: load; S: supernatant; P: pellet.

FIGURE S6: Msps constructs express at the correct molecular weight. Western blot analysis of extracts from *Drosophila* S2 cells transfected with GFP control, Msps TOG1-5-GFP (12345), Msps TOG1-4-GFP (1234), or Msps TOG1-4-GFP with each TOG domain's HR A loop tryptophan mutated to glutamate (1234WE), and probed with anti-GFP antibody. All constructs expressed and ran at their expected molecular weight.

FIGURE S7: EB1 comet length scales with the MT polymerization rate. (A) Fluorescence line scans along MT plus ends measuring the relative EB1-tRFP signal intensity. Shown are averaged line scans from S2 cells 1) treated with control dsRNA and transfected with a GFP control vector (black trace), 2) treated with *msps* dsRNA and transfected with a GFP control vector (red trace), and 3) treated with *msps* dsRNA and transfected with Msps TOG1-4-GFP (green trace). Distance (μm) is measured from the MT plus end towards the minus end. The length of half-maximal intensity comet length is indicated for each trace (μm). (B) The length of half-maximal EB1-tRFP comet intensity (y-axis) is plotted relative to the average velocity of these comets (x-axis). EB1 half-maximal comet length scales linearly with MT plus end velocity, indicating that MT sliding is not disproportionately affecting the various analyses.

FIGURE S8: Model of XMAP215 family proteins at the microtubule plus end. A simplistic model is presented showing an XMAP215 family member with a pentameric TOG array interacting with a MT plus end. The MT plus end is shown as a B-lattice, closed tube, though data suggests that the polymerizing MT plus end may be an open sheet (Mandelkow et al., 1991; Chretien et al., 1995). The TOG domains are colored as in Figure 1A. Given that a conserved tryptophan in the HR A loop of each of the first four TOG domains when mutated to glutamate reduces rescue activity, it is likely that this tryptophan is used by each TOG domain to interact with a tubulin heterodimer as observed in the Stu2 TOG1-αβ-tubulin structure (Ayaz et al., 2012). Thus, each TOG domain is shown interacting with a tubulin heterodimer in the lattice with the polarity observed in the Stu2 TOG1-αβ-tubulin structure: the TOG domain's N- and C-termini directed towards the MT plus and minus end respectively. The model presented is simplistic, and has the full array bound to sequential tubulin subunits along a single protofilament, but whether all TOG domains bind the same protofilament, whether they are arranged from the plus end to the minus end, and what the lateral and longitudinal spacing of each TOG domain on the lattice is remains to be determined. The model, as presented, would position the XMAP215 C-terminal domain (CTD) distal to the MT plus end where it would interact with EB1 via SLAIN2/Sentin. The model does not take into account the curvature of the αβ-tubulin heterodimer observed in the Stu2 TOG1-αβ-tubulin complex, also modeled in our Msps TOG4-αβ-tubulin complex (Fig. 5C). Whether TOG domain binding to the curved tubulin heterodimer occurs only during subunit incorporation and/or to the curved tubulin in a polymerizing protofilament as would be required to transition from an open sheet to a closed lattice remains to be determined. Relative scales are shown at right.

SUPPLEMENTAL MOVIES

MOVIE S1: Msps TOG1-4 and TOG1-5 constructs largely rescue MT polymerization rates. As shown in Figure 8D-G. *Drosophila* S2 cells transfected with EB1-tRFP and GFP (A, B), Msps TOGs 1-4 (C), or Msps TOGs 1-5 (D) were treated with control (A) or *msps* dsRNA (B-D). Normal EB1 comet velocities were found to be 12.2 μm/min (A). Treating with *msps* dsRNA reduces EB1 comet velocities to 2.1 μm/min (B) and rates can be largely rescued by Msps TOGs 1-4 (6.1 μm/min, C) or Msps TOGs 1-5 (6.7 μm/min, D). Images were acquired at 3-second intervals. Only the EB1-tRFP signal is shown.

MOVIE S2: A fully functional TOG array in necessary for the Msps TOG1-4 construct to rescue MT polymerization rates. As shown in Figure 8F, I-O. *Drosophila* S2 cells transfected with EB1-tRFP and a Msps TOG1-4-GFP construct were treated with *msps* dsRNA. A. EB1 comet velocities can be largely rescued with a construct containing only TOGs 1-4. Mutating the conserved HR A loop tryptophan individually in each of the four TOG domain (B-E), in tandem pairs (F-G), or across all four TOG domains (H) impairs the ability of these mutant constructs to rescue EB1 comet velocities. Images were acquired at 3-second intervals. Only the EB1-tRFP signal is shown.

SUPPLEMENTAL REFERENCES

Ayaz, P., Ye, X., Huddleston, P., Brautigam, C.A., and Rice, L.M. (2012). A TOG:αβ-tubulin complex structure reveals conformation-based mechanisms for a microtubule polymerase. Science *337*, 857-860.

Chretien, D., Fuller, S.D., and Karsenti, E. (1995). Structure of growing microtubule ends: two-demensional sheets close into tubes at variable rates. J Cell Biol *129*, 1311-1328.

Mandelkow, E.M., Mandelkow, E., and Milligan, R.A. (1991). Microtubule dynamics and microtubule caps: a time resolved cryo-electron microscopy study. J Cell Biol *114*, 977-991.

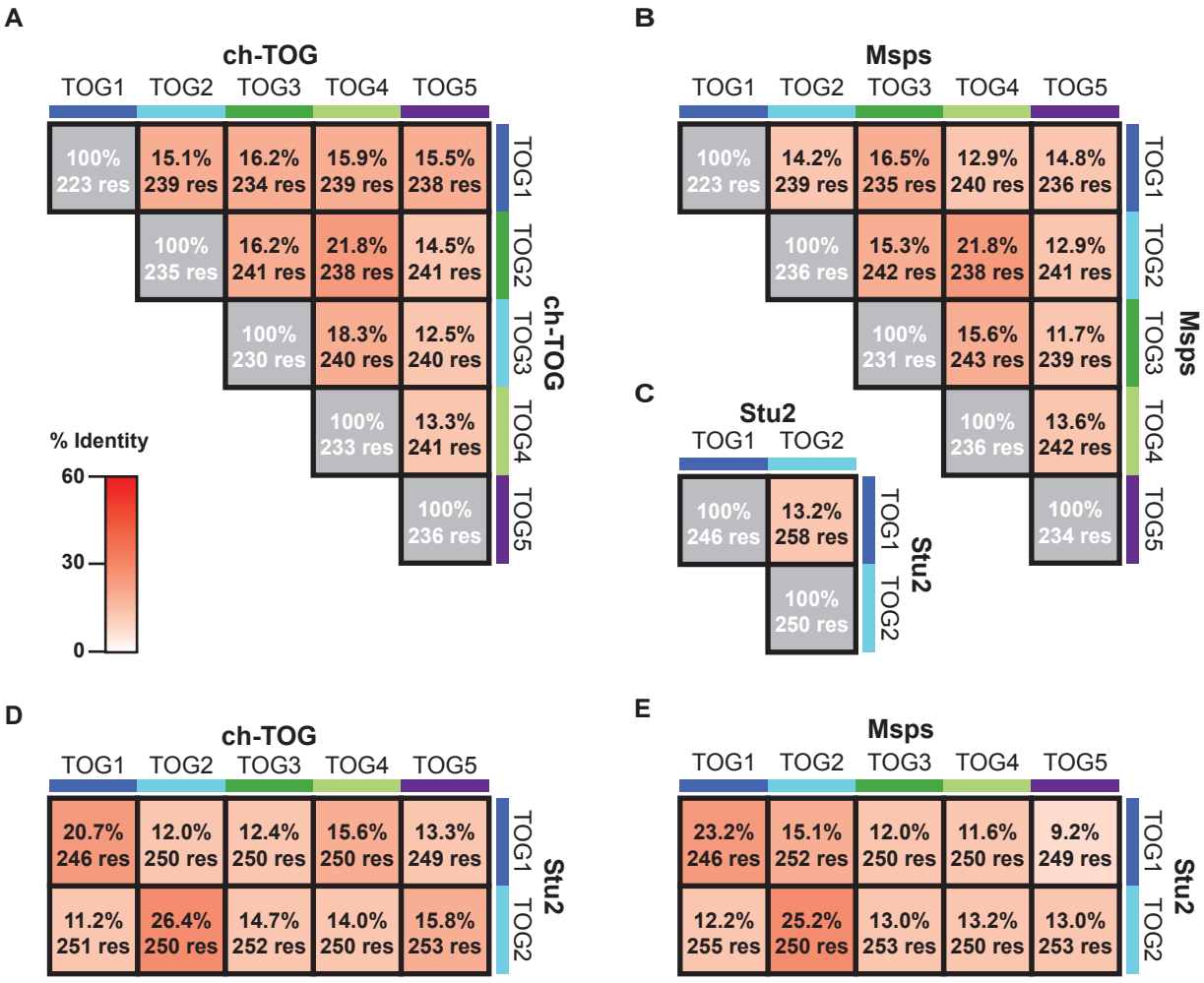

FIGURE S1: TOG domains show positional conservation in the array. (A-E) Identity matrices, comparing TOG domains within a protein (A, ch-TOG; B, Msps; C, Stu2) or across species (D, ch-TOG vs. Stu2; E, Msps vs. Stu2). Percent identity, based on the alignment presented in Figure 1C, is indicated in each cell with the corresponding number of aligned residues listed below. Percent identity is contoured from 0% (white) to 60% (red). 100% identity is shown in gray.

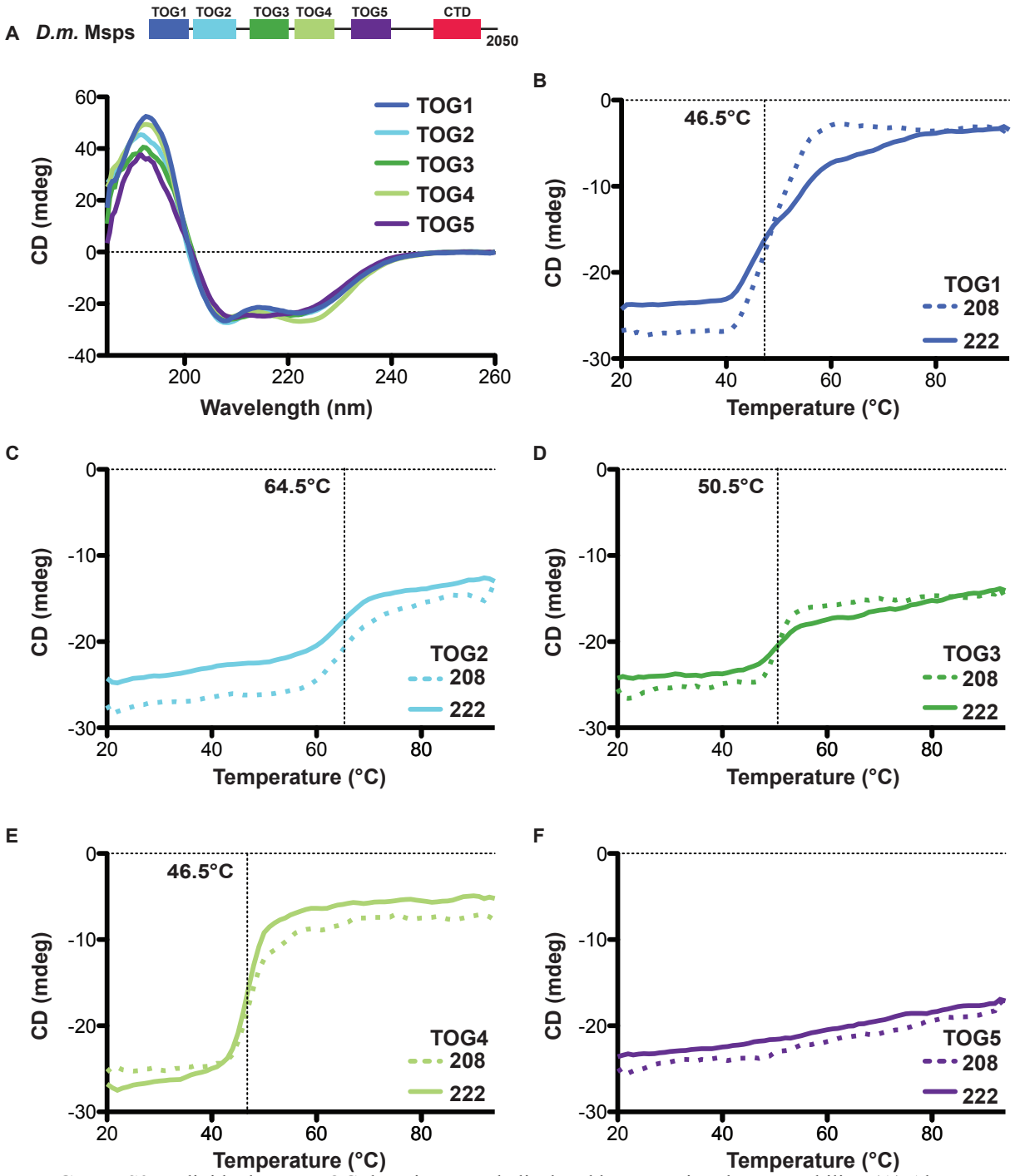

FIGURE S2: Individual Msps TOG domains are α-helical and have varying thermo-stability. (A) Above: domain architecture of *Drosophila* Msps; below: CD spectra of Msps TOG1 (blue), TOG2 (cyan), TOG3 (green), TOG4 (light green), and TOG5 (purple) at 23°C, pH 7.5 (3.7 μM). Spectra show minima at 208 and 222 nm, indicative of α-helical structure in each of the TOG domains. (B-F) CD melts of Msps TOG1 (B), TOG2 (C), TOG3 (D), TOG4 (E), and TOG5 (F). CD signal was monitored at 208 nm (dashed trace) and 222 nm (solid trace) in 1°C steps from 20°C to 94°C. The inflection points were 46.5°C, 64.5°C, 50.5°C, and 46.5°C for TOG1, TOG2, TOG3, and TOG4, respectively. TOG5 had no inflection point suggesting that the domain, as defined by the region exclusively spanning its six predicted HEAT repeats, is not stable. Experiments were performed in duplicate with data from single, representative experiments shown.

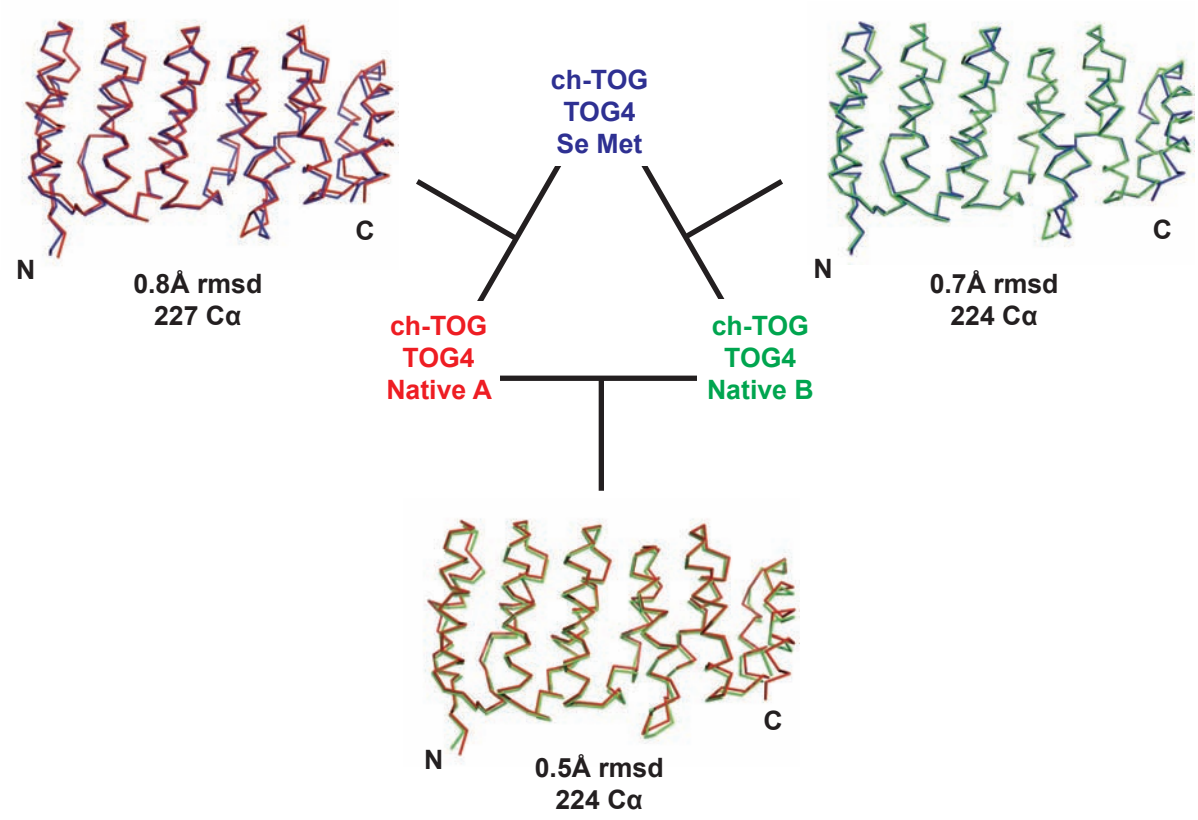

FIGURE S3: TOG4 protomer structures are similar within and across space groups. Pairwise structural alignment of human ch-TOG TOG4 determined in two different crystal forms (ch-TOG TOG4 SeMet, $P4_32_12$ (blue); ch-TOG TOG4 native, $P2_12_12_1$ protomer A (red), ch-TOG TOG4 native, $P2_12_12_1$ protomer B (green). Cα rmsd values are indicated below each alignment with the corresponding number of Cα atoms aligned.

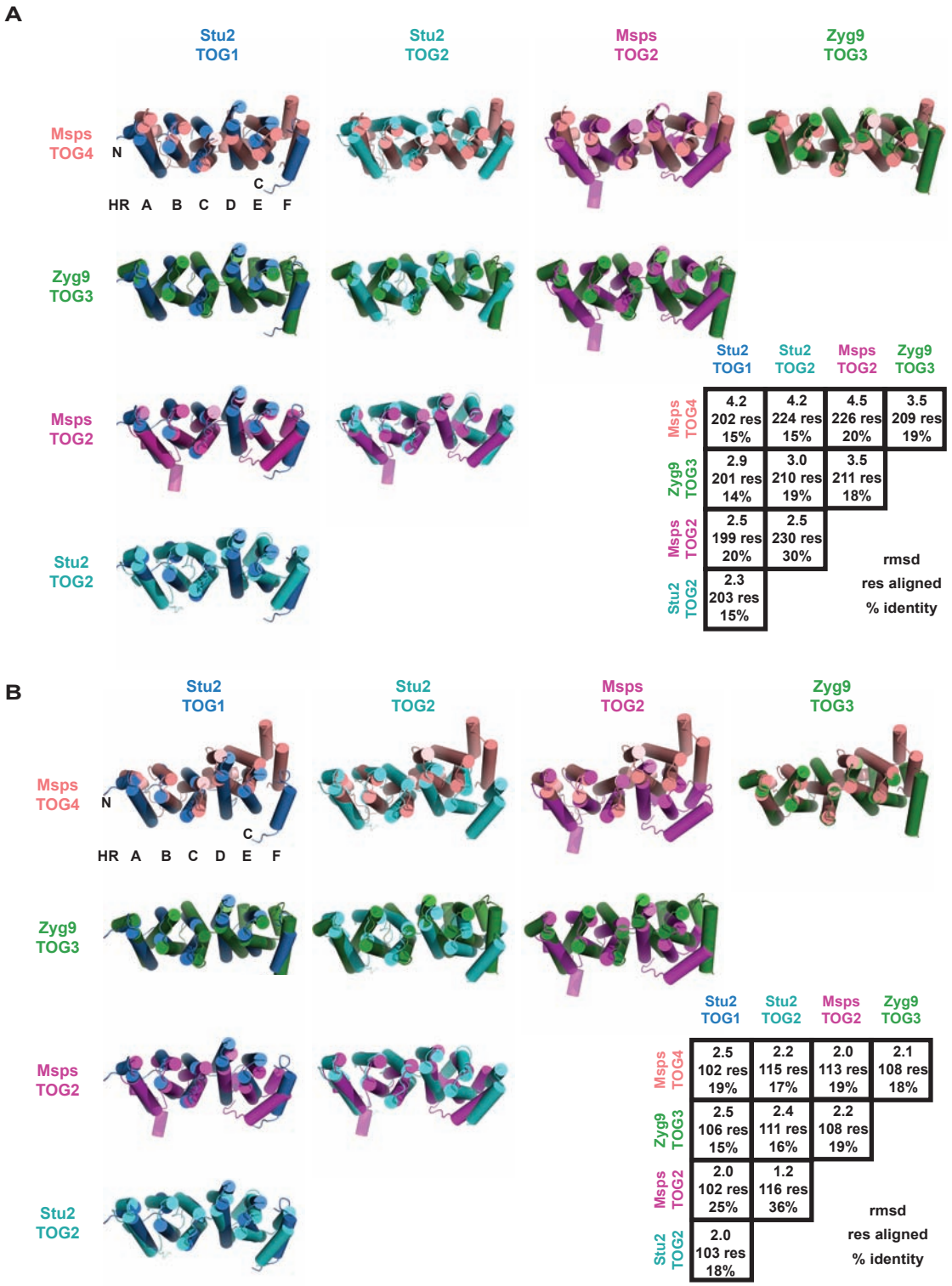

FIGURE S4: The TOG4 structure is architecturally distinct from other XMAP215 TOG structures. Pairwise structural alignment matrix of XMAP215 family TOG domains: Stu2 TOG1 (dark blue), Stu2 TOG2 (cyan), Msps TOG2 (purple), Zyg-9 TOG3 (green), and Msps TOG4 (pink). Domains are shown in cartoon representation. Matrices in the lower right indicate the rmsd values (top) for the number of Cα atoms aligned (center), and the percent identity across the aligned region (bottom). (A) Pairwise structural alignment performed across HR A-F. (B) Pairwise structural alignment performed across HR A-C.

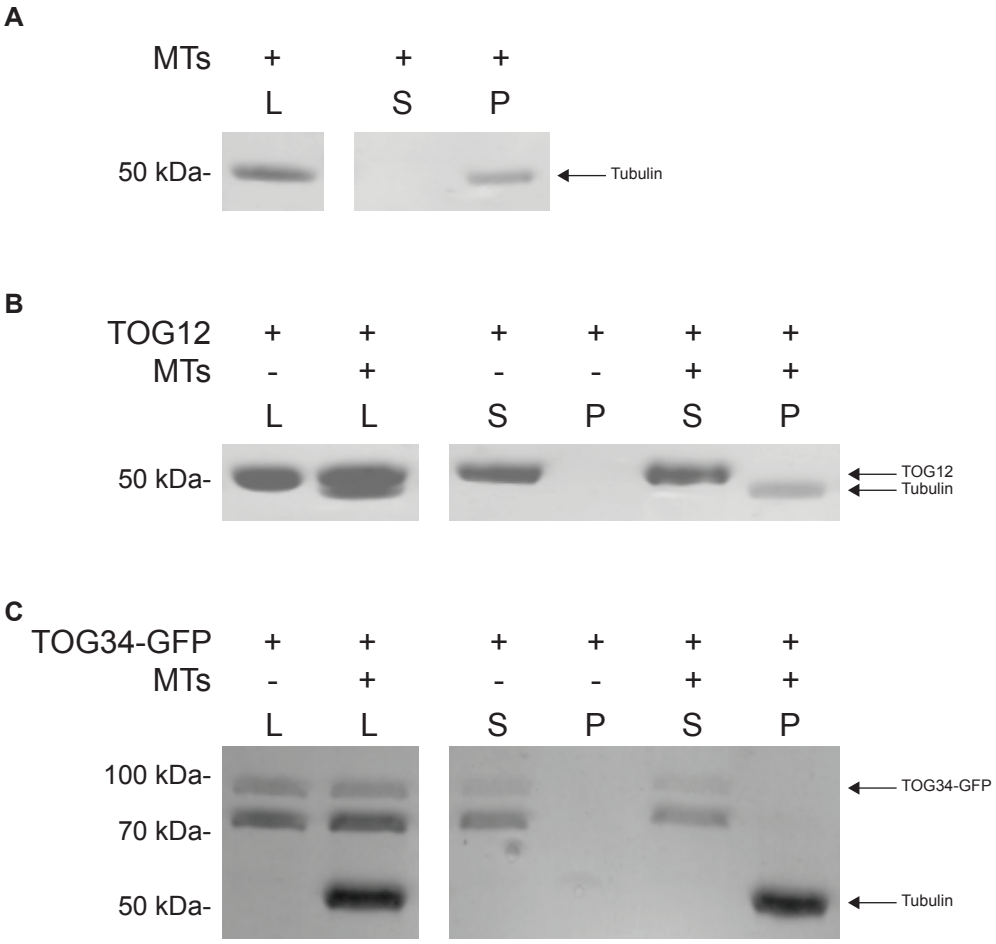

Figure S5: Msps TOG12 and TOG34 do not co-sediment with taxol-stabilized MTs. (A) MTs were pelleted at 100,000xg. 100% of the load (left panel) was observed in the pellet (right panel, right lane). A Msps TOG12 construct (residues 1-516) (B) and a TOG34-GFP construct (residues 582-1080, upper band; lower band is a TOG34-GFP degradation product) (C) were centrifuged in the presence and absence of taxol-stabilized MTs (left panels, load; right panel supernatant and pellets). Both constructs were observed in the supernatant alone indicating that the constructs, at the concentrations used, do not robustly bind and co-sediment with taxol-stabilized MTs. L: load; S: supernatant; P: pellet.

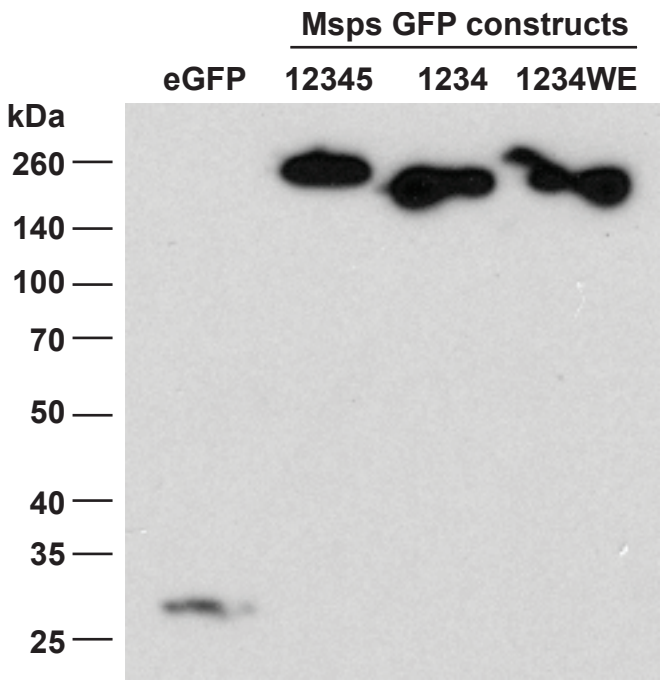

FIGURE S6: Msps constructs express at the correct molecular weight. Western blot analysis of extracts from *Drosophila* S2 cells transfected with GFP control, Msps TOG1-5-GFP (12345), Msps TOG1-4-GFP (1234), or Msps TOG1-4-GFP with each TOG domain's HR A loop tryptophan mutated to glutamate (1234WE), and probed with anti-GFP antibody. All constructs expressed and ran at their expected molecular weight.

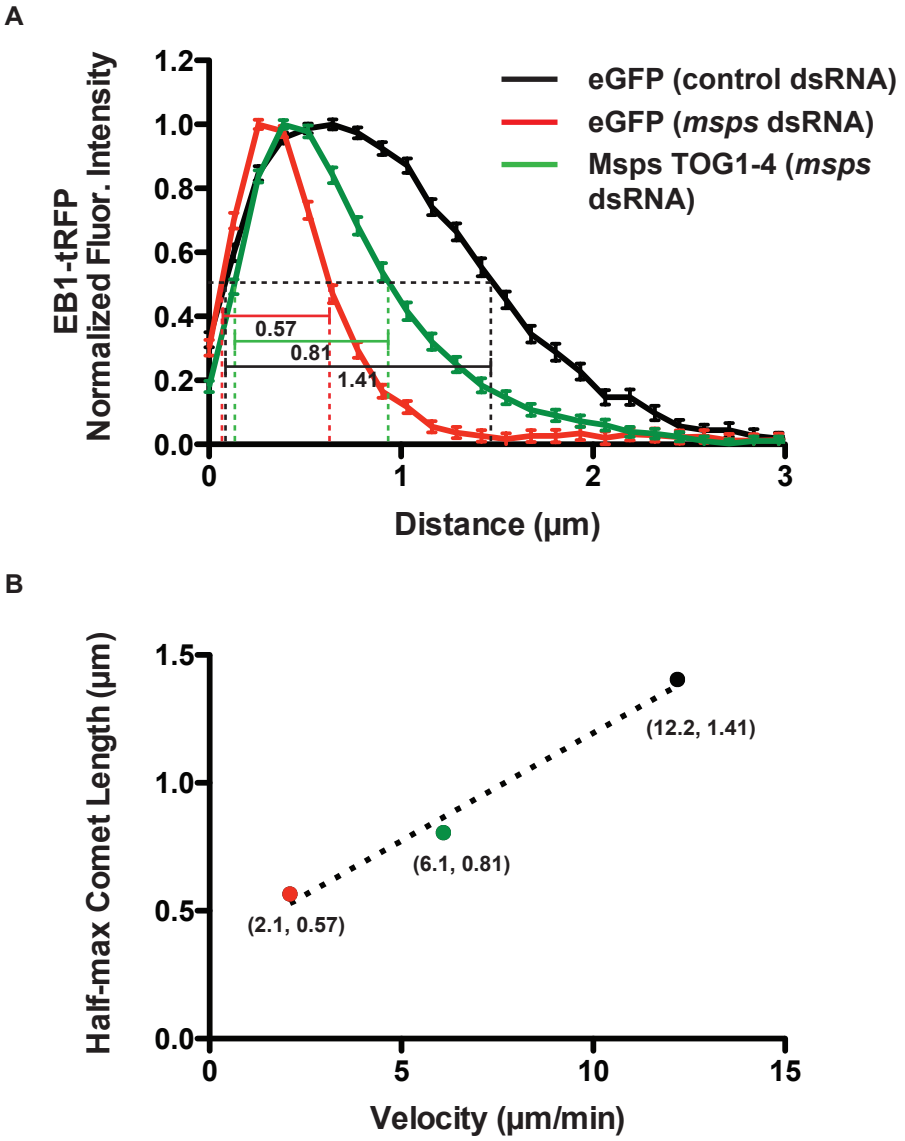

FIGURE S7: EB1 comet length scales with the MT polymerization rate. (A) Fluorescence line scans along MT plus ends measuring the relative EB1-tRFP signal intensity. Shown are averaged line scans from S2 cells 1) treated with control dsRNA and transfected with a GFP control vector (black trace), 2) treated with *msps* dsRNA and transfected with a GFP control vector (red trace), and 3) treated with *msps* dsRNA and transfected with Msps TOG1-4-GFP (green trace). Distance (µm) is measured from the MT plus end towards the minus end. The length of half-maximal intensity comet length is indicated for each trace (µm). (B) The length of half-maximal EB1-tRFP comet intensity (y-axis) is plotted relative to the average velocity of these comets (x-axis). EB1 half-maximal comet length scales linearly with MT plus end velocity, indicating that MT sliding is not disproportionately affecting the various analyses.

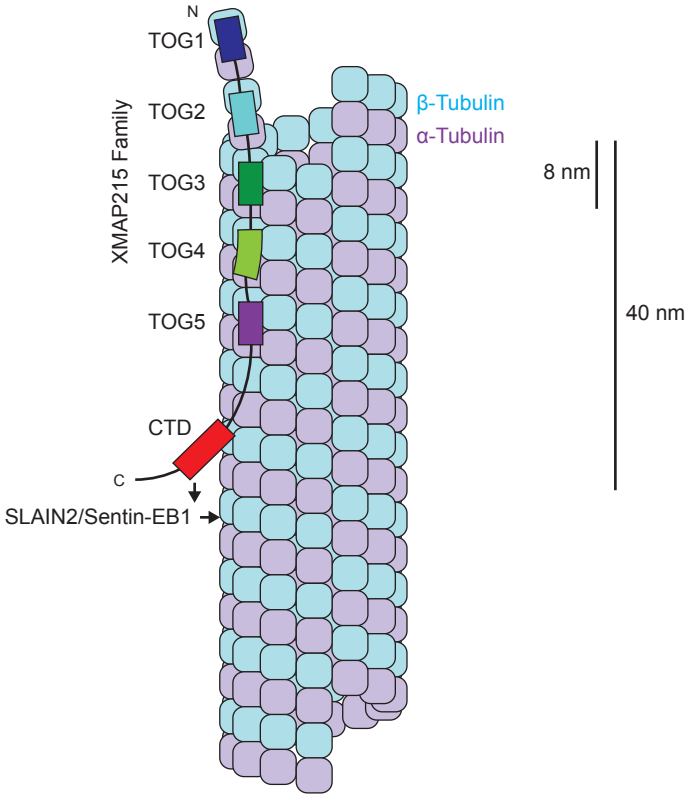

FIGURE S8: Model of XMAP215 family proteins at the microtubule plus end. A simplistic model is presented showing an XMAP215 family member with a pentameric TOG array interacting with a MT plus end. The MT plus end is shown as a B-lattice, closed tube, though data suggests that the polymerizing MT plus end may be an open sheet (Mandelkow et al., 1991; Chretien et al., 1995). The TOG domains are colored as in Figure 1A. Given that a conserved tryptophan in the HR A loop of each of the first four TOG domains when mutated to glutamate reduces rescue activity, it is likely that this tryptophan is used by each TOG domain to interact with a tubulin heterodimer as observed in the Stu2 TOG1-αβ-tubulin structure (Ayaz et al., 2012). Thus, each TOG domain is shown interacting with a tubulin heterodimer in the lattice with the polarity observed in the Stu2 TOG1-αβ-tubulin structure: the TOG domain's N- and C-termini directed towards the MT plus and minus end respectively. The model presented is simplistic, and has the full array bound to sequential tubulin subunits along a single protofilament, but whether all TOG domains bind the same protofilament, whether they are arranged from the plus end to the minus end, and what the lateral and longitudinal spacing of each TOG domain on the lattice is remains to be determined. The model, as presented, would position the XMAP215 C-terminal domain (CTD) distal to the MT plus end where it would interact with EB1 via SLAIN2/Sentin. The model does not take into account the curvature of the αβ-tubulin heterodimer observed in the Stu2 TOG1-αβ-tubulin complex, also modeled in our Msps TOG4-αβ-tubulin complex (Fig. 5C). Whether TOG domain binding to the curved tubulin heterodimer occurs only during subunit incorporation and/or to the curved tubulin in a polymerizing protofilament as would be required to transition from an open sheet to a closed lattice remains to be determined. Relative scales are shown at right.